A New Deep-Beam Element for Mixed-Type Modeling of Concrete Structures

Jian Liu, Ph.D. Candidate, Liège

Dr. Serhan Guner, Assistant Professor, Toledo

Dr. Boyan Mihaylov, Assistant Professor, Liège

Department of ArGEnco, University of Liège, Belgium

Department of Civil Engineering, The University of Toledo, Ohio, USA

(This research was conducted in 2016; this report was released in 2021.)

Contents

1 Introduction 1

1.1 What are deep beams? 1

1.2 Problems with modelling large frame structures with deep beams included 1

1.3 Solution proposed 2

2 Formulation of a Deep-Beam Element based on 3PKT 2

2.1 Brief introduction on 3PKT 2

2.2 Formulation of 1D deep element 3

2.3 Solution scheme of 1D deep element 5

2.4 Subroutine DPBM for 1D deep element 6

2.5 Adaption of the deep element into VecTor5 7

3 A New Member Type in VecTor5 7

3.1 Description of Type-8 member 7

3.2 User guide: implementation of Type-8 member 7

3.3 Shear protection 8

3.4 Output files 9

4 Verification studies 9

4.1 Simply supported beams 10

4.1.1 1st set of tests: Salamy (2005) 10

4.1.2 2nd set of tests: Tanimura (2005) 19

4.2 Continuous deep beam 22

4.3 Frames 23

4.3.1 Two-story single-span frame 23

4.3.2 Two-story two-bay frame 27

4.3.3 Force control vs. displacement control 28

5 Future Work 30

5.1 Axial force 30

5.2 Unloading/reloading path 30

5.3 Automatic detection of deep beam element 30

5.4 Output of crack pattern in Janus 30

6 References 30

Annex 1: Flow chart of subroutine DPBM 31

1 Introduction

1.1 What are deep beams?

Deep beams are typically used as transfer girders in high-rise buildings or bridges. An example is shown in Figure 1, where a deep transfer girder is used to carry the heavy loads from upper stories to have an open space at the lower story of a large frame structure. The shear-span-to depth ratio a/d for deep beam is much lower than slender beam, which attributes to the difference in shear behaviour between these two types of beams. Generally, if a/d is less than 2.5, the beam is considered to be deep; otherwise, it is slender. Due to this characteristic, deep beams have disturbed deformation field and do not obey the assumption of classical beam theory, i.e., 'plane section remain plane'.

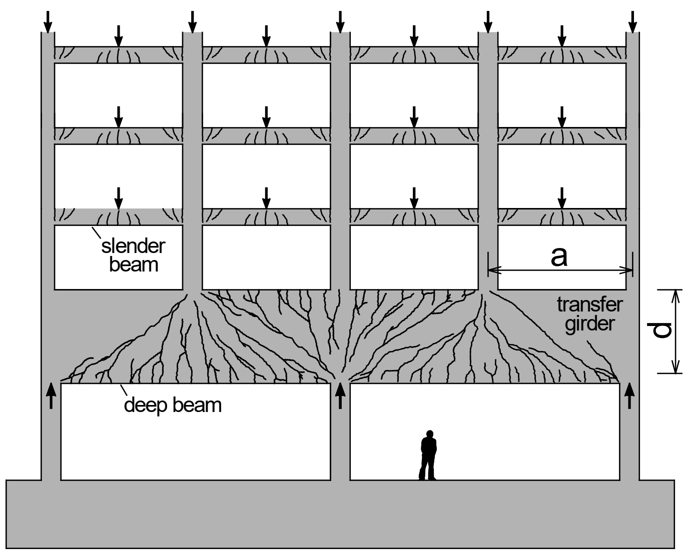

Figure 1: Typical large frame structure with deep beams.

1.2 Problems with modelling large frame structures with deep beams included

A frame structure can be modelled either with 1D frame element (e.g., in VecTor5) or with 2D element (e.g., in VecTor2, see Figure 2). The former holds advantage over the latter due to its efficiency in model formation and calculation as well as its good compatibility with other elements. However, 1D frame elements are formulated based on the slender beam theory, and thus cannot provide accurate predictions for deep beams. Despite its inefficiency, 2D element is able to provide relatively accurate predictions. Therefore, it is not an easy task to model a large frame with deep beams included efficiently and accurately.

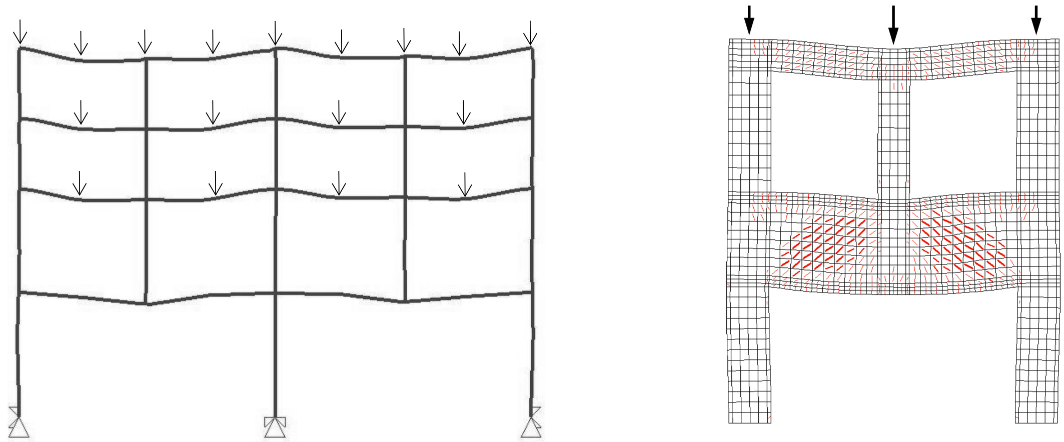

(a) Model with 1D frame element (VecTor5) *(b) Model with 2D element (VecTor2)*

Figure 2: Typical large frame structure with deep beams.

1.3 Solution proposed

One of the solutions to the problem described in 1.2 is to formulate a 1D element especially for deep beams to combine efficiency as in 1D frame elements and, at the same time, accuracy comparable to that of 2D elements. This 1D element should be compatible with other types of elements as well, to make it possible to have a mixed-type structure with both 1D deep and slender elements as shown in Figure 1. More specifically, the final objective of this research is to formulate a new type 1D element for deep beams and implement this into the frame analysis procedure VecTor5.

2 Formulation of a Deep-Beam Element based on 3PKT

2.1 Brief introduction on 3PKT

A two-span continuous deep beam is tested in the University of Toronto in 2012 (Mihaylov et al., 2015) as shown in Figure 3. It can be seen the at failure the shear span is divided by a diagonal crack which runs from the corner (edge of the loading column) to corner (the edge of support column), and at the same time there are some minor cracks radiating from the two corners to the longitudinal reinforcements at section bottom or top. Based on this observation, Mihaylov et al. proposed a three-parameter kinematic theory (3PKT), in which the shear span is considered consisting of two fans separated by a straight diagonal crack. The openings of the two fans are related to the elongation of the longitudinal reinforcements ε_{t1} and ε_{t2} (see Figure 4). At the same time, the two fans translate vertically from each other due to the localized compressive deformation Δ_c in a so-called area “critical loading zone” (CLZ) which is located at one tip of the fan. The complete deformation pattern is the superposition of the two basic deformation patterns. Refer to Mihaylov (2013) for more details.

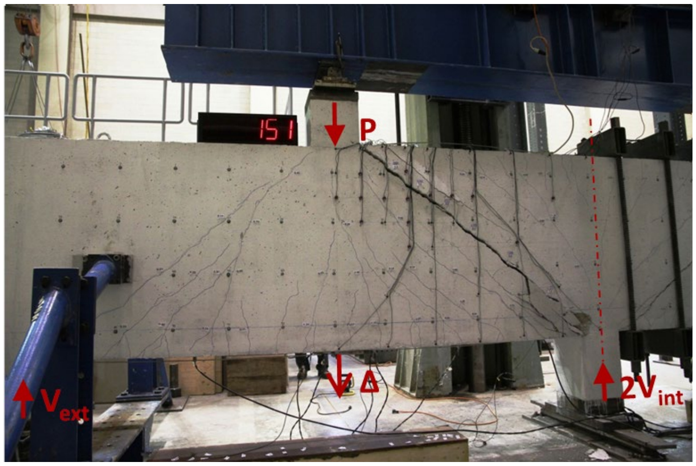

Figure 3 Deep beam at failure.

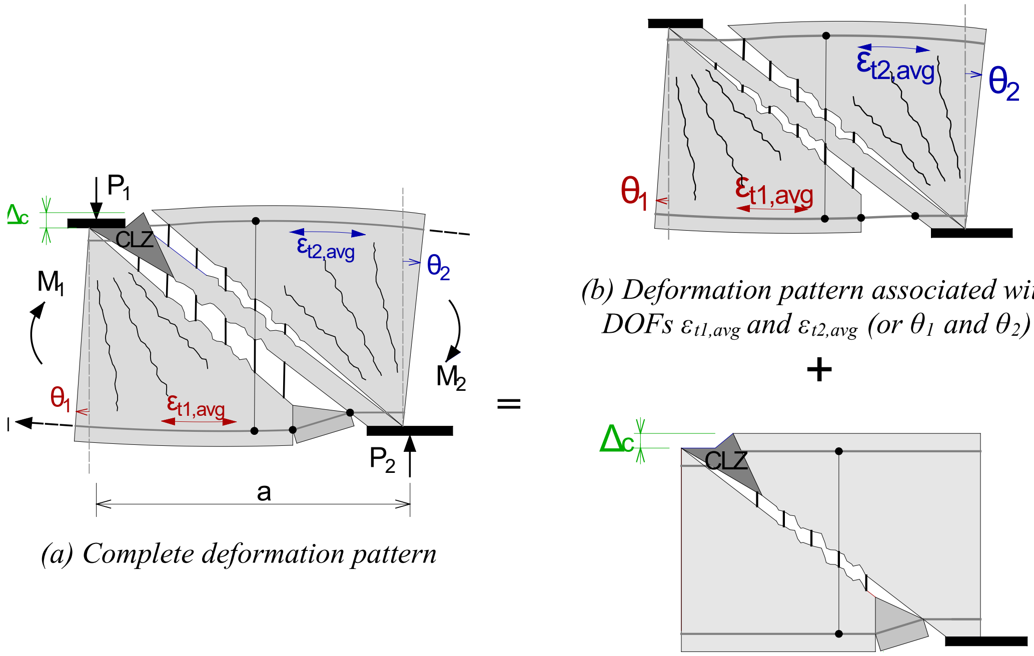

(a) Complete deformation pattern

(b) Deformation pattern associated with DOFs $\varepsilon_{t1,avg}$ and $\varepsilon_{t2,avg}$ (or θ_1 and θ_2)

(c) Deformation pattern associated with DOF Δ_c

Figure 4 Three-parameter kinematic model for shear spans of deep beams under double curvature

2.2 Formulation of 1D deep element

3PKT provides another option for deep beam analysis, and in fact compared with other theories or models, e.g., strut-and-tie model, plasticity model; it is more suitable for the formulation of 1D element. As demonstrated in Figure 5, the two fans can be lumped as two rotational springs and the rotations are equivalent to the opening angle of the two fans (θ_1 and θ_2). The deformation in CLZ Δ_c can be equivalent to the elongation in a transverse spring located at the mid-shear-span. The transverse spring, in fact, consists of four parallel springs which correspond to the four shear mechanisms considered in 3PKT. There are two DOF at each node, i.e., sectional rotation and vertical displacement. The secant stiffness of the three springs is k_1, k_2 and k_3, respectively.

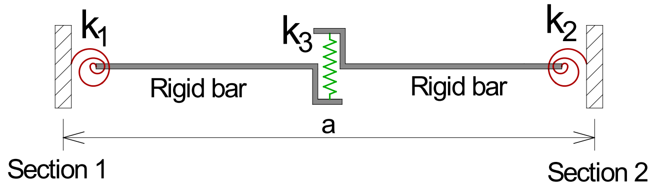

(a) Components of the macro-element

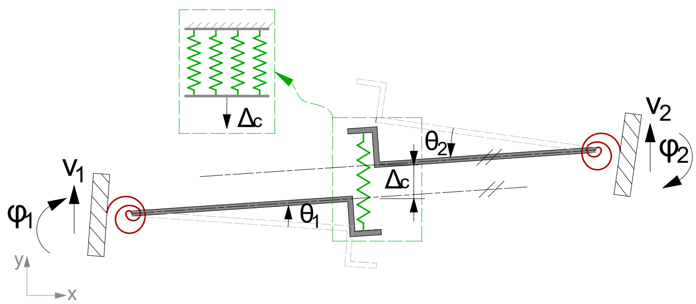

(b) Kinematics of the macro-element

Figure 5 Macro element for deep shear spans

Therefore, the stiffness matrix of this 1D deep element can be written as:

$$[k]=\frac{1}{k_1+k_2+k_3a^2}\times\begin{bmatrix} k_1\left(k_2+k_3a^2\right) & -k_1k_3a & -k_1k_2 & k_1k_3a \\ -k_1k_3a & k_3\left(k_1+k_2\right) & -k_2k_3a & -k_3\left(k_1+k_2\right) \\ -k_1k_2 & -k_2k_3a & k_2\left(k_1+k_3a^2\right) & k_2k_3a \\ k_1k_3a & -k_3\left(k_1+k_2\right) & k_2k_3a & k_3\left(k_1+k_2\right) \end{bmatrix} \tag{1}$$

Once the stiffness matrix and boundary condition are known, the shear span can be solved with the following equation:

$$\begin{Bmatrix} M_1 \\ V \\ M_2 \\ -V \end{Bmatrix}=[k]\begin{Bmatrix} \varphi_1 \\ v_1 \\ \varphi_2 \\ v_2 \end{Bmatrix} \tag{2}$$

This 1D deep element is easy being connected with other element either of the same type or different type. Deep beams can be easily modelled by connecting two or more 1D deep element as shown in Figure 6 Macro-element model of a continuous deep beam.

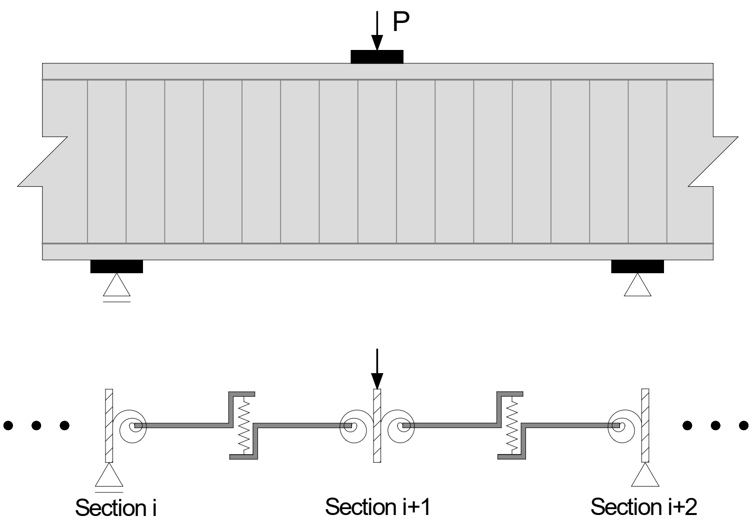

Figure 6 Macro-element model of a continuous deep beam

2.3 Solution scheme of 1D deep element

Since the secant stiffness of the springs of the macro element changes with the level of loading, an iterative solution procedure is required to achieve equilibrium between the internal and external forces at each load stage. The linear system expressed with Eq. (2) can be first solved with a selected set of secant stiffnesses, for instance those from the previous converged load stage. This analysis produces deformations θ_1, θ_2 and Δ_c in the springs of each macro element, and these deformations are substituted to calculate new values of the forces in the springs M_1, M_2 and V. These forces are in turn used to calculate new secant stiffnesses $k_1=M_1/\theta_1$, $k_2=M_2/\theta_2$ and $k_3=V/\Delta_c$ with which to perform the next linear elastic analysis. The procedure is repeated until the secant stiffnesses of the springs converge to constant values. The iterations for a transverse spring in a typical deep beam analysis are demonstrated in Figure 7. The crosses in the plot show two consecutive converged load stages, while the inclined lines show the secant stiffness as it changes from iteration to iteration. The displacement Δ_c obtained from each linear analysis is marked with a vertical line. The intersection point between the vertical line and the V-Δ_c curve is used to define the secant stiffness for the next iteration. As the iterations progress, the vertical lines become progressively closer until the solution converges.

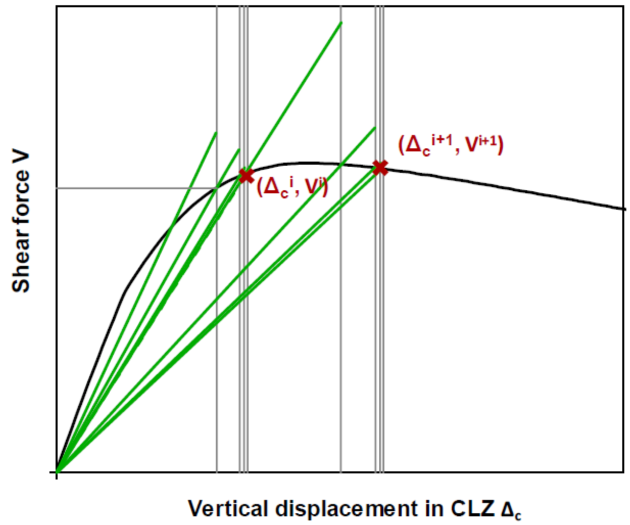

Figure 7 Iteration scheme demonstrated for a transverse spring.

2.4 Subroutine DPBM for 1D deep element

Based on the description in the previous section, a subroutine is developed for the deep element. This subroutine has the displacements at each node as inputs. It should be noticed that those displacements are in global coordinate system and need to be transformed into the DOF in local coordinate system for each shear span. At the same time there is one more DOF included which is the axial displacement of the node, i.e., u. The axial behaviour of the deep element is assumed to be elastic, i.e., $N = E_c A_g u/L$. Therefore, the outputs are the axial force AF, shear force BF and bending moment SM. It can be expressed in Figure 8.

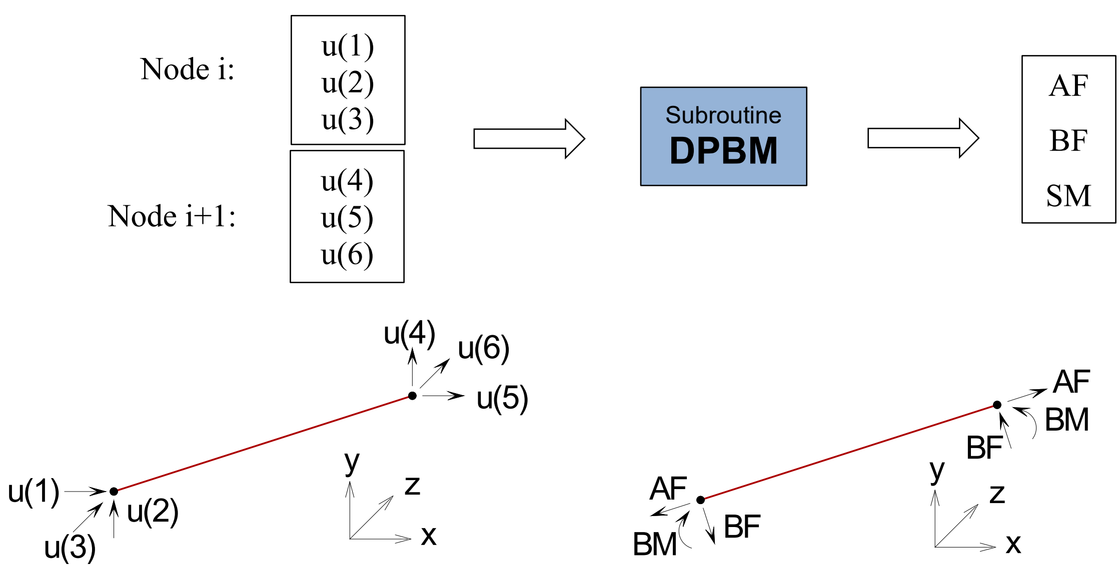

Figure 8 The function of subroutine DPBM

2.5 Adaption of the deep element into VecTor5

Generally, the bending moments at two ends of the deep element, i.e., M_1 and M_2, are not equal (see Equation 2), however, in order to be adapted to the framework of VecTor5, the bending moment calculated by subroutine DPBM is taken as $BM=(M_1-M_2)/2$. At the same time dowel action is considered explicitly in subroutine DPBM, therefore, the dowel action in original VecTor5 is skipped in the calculation of shear capacity of deep members. Details are not meant to be mentioned in this report.

3 A New Member Type in VecTor5

3.1 Description of Type-8 member

There are seven existing member types in VecTor5, including: nonlinear frame member (default member), truss member, tension-only member, compression-only member, etc. A new member type for nonlinear deep member is added into VecTor5, named as 'Type 8 member'. Similar to the nonlinear frame member (see Figure 9), the new-type member has three DOFs at each node; i.e., axial displacement, transverse displacement and rotation in the local coordinate system.

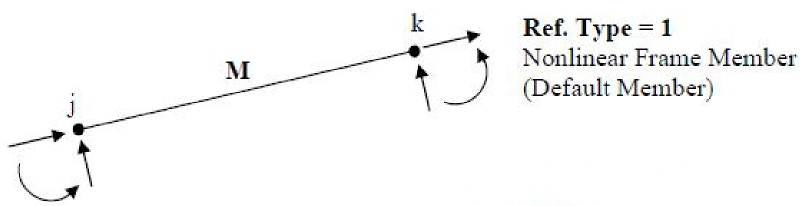

(a) Default nonlinear frame member

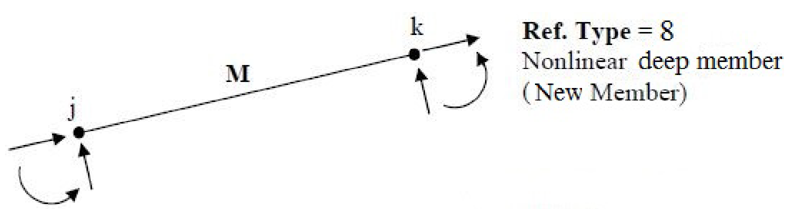

(b) New nonlinear deep member

Figure 9 Member reference types in VecTor5

3.2 User guide: implementation of Type-8 member

The user should make the decision if there is any deep member in the model. This member should be defined as Type 8, as shown in Figure 10. All the input files (*.s5r, *.l5r, *.job and

*.aux) are created in the same manner as in the original VecTor5 except the following two aspects. See *Bulletin 8: Deep Beam Modeling with VecTor5* <web link> for more information.

1) If Type-8 member is to be used, only one element should be used for one shear span. There is no need to discretize the shear span.

2) It is necessary to provide data on the loading plate/support width since this is an important parameter when determining the shear contribution from critical loading zone calculated in the subroutine DPBM. The required input is shown in Figure 10.

```
                      (D) Member Specifications
                      -------------------------
 MT      f'c   [ f't     Ec       e0      Mu      Cc       Kc      Agg    Dens]   [Smx    Smy]
        (MPa)  (MPa)   (MPa)    (me)           (/deg.C)  (mm2/hr)  (mm)  (kg/m3)   (mm)   (mm)
   1   27.00   0.000   0.000   0.000   0.000   0.000    0.000   20.000   0.000   0.000   0.000
   2   27.00   0.000   0.000   0.000   0.000   0.000    0.000   20.000   0.000   0.000   0.000
/

 MT     Nc      Ns      Fyz      St       Dbt      Fyt      Fut        Est        esht     eut      Cs     Ref
        (#)     (#)    (MPa)    (mm)     (mm)     (MPa)    (MPa)      (MPa)       (me)     (me)  (/deg.C) Type
   1    42      2     400.000  100.000  11.284   400.000  540.000  200000.000   8.000   80.000   0.000    1
   2    42      2     400.000  100.000  11.284   400.000  540.000  200000.000   8.000   80.000   0.000    8
/
```

(a) Ref. Type=8 for deep element

```
VecTor.DPBM - Notepad
File  Edit  Format  View  Help
        * * * * * * * * * * * * * * * * * * *
        *          V e c T o r 5            *
        *     DEEP BEAM ELEMENT PARAMETERS  *
        * * * * * * * * * * * * * * * * * * *

Member Direction LB1(mm) LB2(mm) LB1E(mm) LB2E(mm)/
   1       1       600     800     300      800/
   2       2       600     800     300      800/
/
```

(b) Loading plate/support width input

Figure 10 Input related to the Type-8 members.

3.3 Shear protection

Shear protection is a scheme in VecTor 5 for approximately suppressing premature failures in D-regions (disturbed regions). The new Type-8 member explicitly calculates the shear capacity of deep members; thus, eliminating the need for this scheme. Therefore, it is necessary to turn off shear protection for Type-8 members. To expedite this, the new subroutines automatically turn off shear protection for Type-8 members. The user could see the list of members for which the shear protection on in the *.s5E expanded data file.

3.4 Output files

The results for Type-8 members are shown in the output files as shown in Figure 11. The three kinematic parameters in 3PKT and the corresponding internal forces are listed at the beginning, which is followed by the four shear components. The straight diagonal crack is described with its inclined angle, slip along the crack as well as the crack opening at the mid-length of the crack.

```
                  DEEP BEAM ELEMENT RESULTS
                  *************************

     MOMENT1:    -1.2 kN-m          THETA1   -0.00 milli-rad
     MOMENT2:   121.5 kN-m          THETA2    0.25 milli-rad
       SHEAR:  -601.7 kN            DELTAC    2.52 mm

                    SHEAR RESISTANCE FORCES
                    -----------------------

         VCLZ          VS           VCI          VD
         (KN)         (KN)          (KN)        (KN)

       220.09         0.00        219.49      162.08

                       CRACK CONDITIONS
                       ----------------

          ANGLE      SLIP       WCR AT H/2
          (deg)      (mm)          (mm)

          66.04      2.30          1.05
```

Figure 11 Output related with Type-8 member.

4 Verification studies

Note: Below sections discuss preliminary verification studies using a force-controlled loading protocol. Refer to the following publication for the final results, which uses a displacement-controlled protocol. Liu, J., Guner, S., and Mihaylov, B. (2019) “Mixed-Type Modeling of Structures with Slender and Deep Beam Elements” *ACI Structural Journal*, 116(4), pp. 253-264. <web link>

4.1 Simply supported beams

4.1.1 1st set of tests: Salamy (2005)

The first group of specimens from Salamy (2005 are under symmetrical 4-point bending (see Figure 12). The external two spans sustain high shear while the middle span is under pure flexure. The information of the specimens is listed in Table 1.

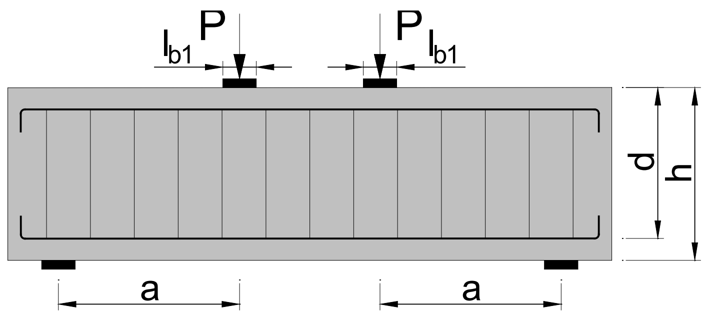

Figure 12 Specimens tested by Salamy (2005)

Table 1 Investigated specimens from Salamy (2005)

Beam	a/d	l_{b1} (mm)	b (mm)	d (mm)	ρ_l (%)	n_b	fy (MPa)	a (mm)	V/P	h (mm)	a_g (mm)	f_c (MPa)	ρ_v (%)	f_{yv} (MPa)	V_{exp} (kN)	Δ_{exp} (mm)	$\frac{V_{exp}}{V_{pred1}}$	$\frac{\Delta_{exp}}{\Delta_{pred1}}$	$\frac{V_{exp}}{V_{pred2}}$	$\frac{\Delta_{exp}}{\Delta_{pred2}}$	$\frac{V_{exp}}{V_{pred3}}$	$\frac{\Delta_{exp}}{\Delta_{pred3}}$
B-10-2	1.50	100	240	400	2.02	5	376	600	1.0	475	20	23.0	0.00	-	357	6.9	0.22	0.43	0.47	0.25	0.73	0.48
B-13-2	1.50	200	480	800	2.07	10	398	1200	1.0	905	20	24.0	0.00	-	1128	9.0	0.13	0.43	0.40	0.13	0.92	0.66
B15	1.50	300	720	1200	1.99	18	402	1800	1.0	1305	20	27.0	0.00	-	2709	16.0	0.09	0.33	0.37	0.10	0.87	0.58
B17	1.50	250	600	1000	2.04	14	398	1500	1.0	1105	20	28.7	0.40	398	2597	11.8	0.44	0.50	0.80	0.89	0.90	0.87
B18	1.50	350	840	1400	2.05	18	398	2100	1.0	1505	20	23.5	0.40	398	4214	16.3	0.24	0.40	0.78	0.70	1.00	0.86
																Avg=	0.22	0.42	0.57	0.41	0.89	0.69
																COV=	60.3%	14.1%	36.8%	87.5%	11.3%	25.0%

Force-control loading is adopted in the modelling to remain under the same condition as in the experiment.

1) Model 1 in original VecTor5

Modelling the full beam with slender elements:

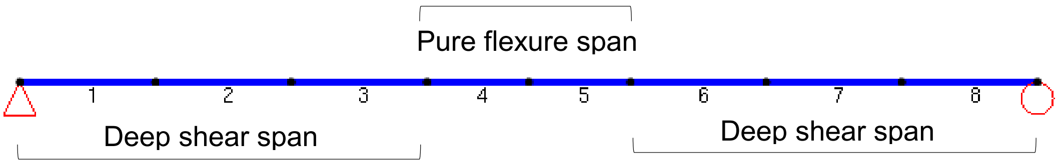

Figure 13 Model in original VT5

All options are kept as default which is the common situation for users.

2) Model 2 in modified VecTor5

Modeling the deep shear spans with deep elements, the pure flexure span with slender elements:

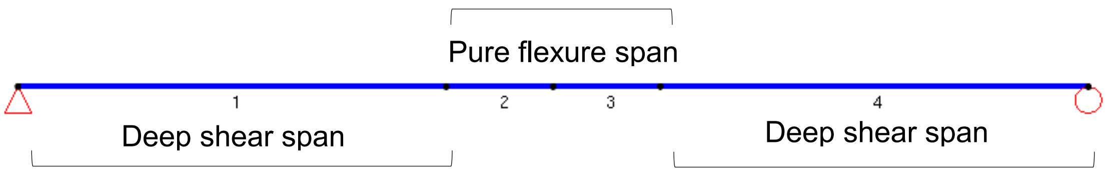

Figure 14 Model in modified VT5

3) Comparison between Model 1 and Model 2

<u>Crack pattern at the same load stage</u>.

Noted that the crack pattern from model 2 is not reliable since the post-processor Janus is not modified for displaying deep beam crack patterns yet.

Table 2 Crack pattern comparison between Model 1 and Model 2 at the same load stage

Beam	Model	Crack pattern
B-10-2	Model 1 (Original VecTor5)	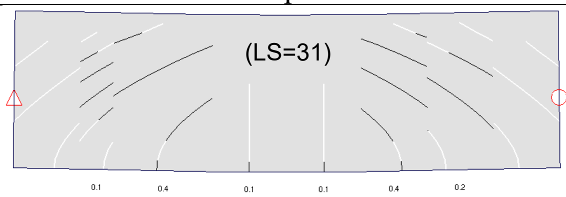
	Model 2 (Modified VecTor5)	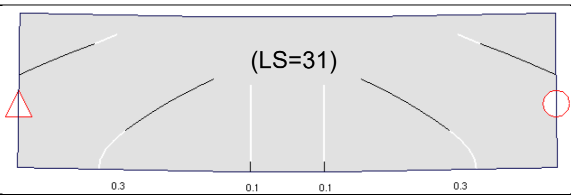

<table>
<tr><td rowspan="2">B-13-2</td><td>Model 1
(Original
VecTor5)</td><td>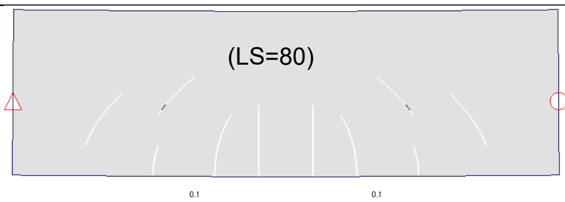
</td></tr>
<tr><td>Model 2
(Modified
VecTor5)</td><td>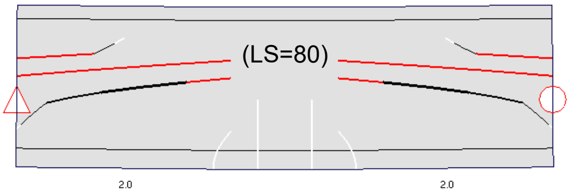
</td></tr>
<tr><td rowspan="2">B15</td><td>Model 1
(Original
VecTor5)</td><td>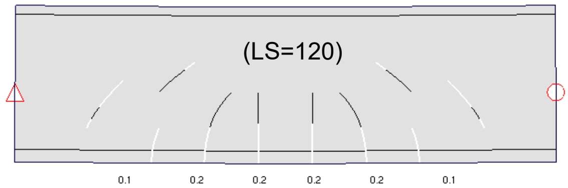
</td></tr>
<tr><td>Model 2
(Modified
VecTor5)</td><td>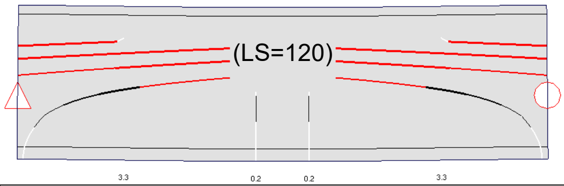
</td></tr>
<tr><td rowspan="2">B17</td><td>Model 1
(Original
VecTor5)</td><td>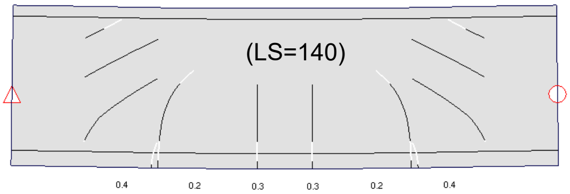
</td></tr>
<tr><td>Model 2
(Modified
VecTor5)</td><td>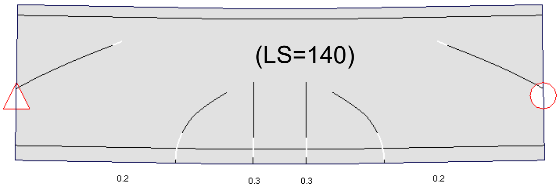
</td></tr>
<tr><td rowspan="2">B18</td><td>Model 1
(Original
VecTor5)</td><td>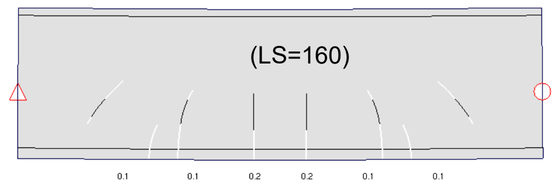
</td></tr>
<tr><td>Model 2
(Modified
VecTor5)</td><td>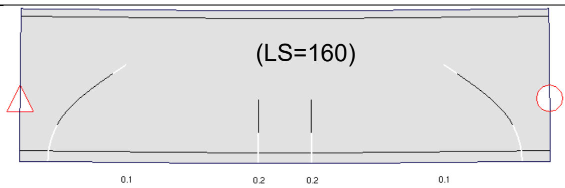
</td></tr>
</table>

Crack pattern at failure

Table 3 Crack pattern comparison between Model 1 and Model 2 at failure

Beam	Model	Crack pattern
B-10-2	Model 1 (Original VecTor5)	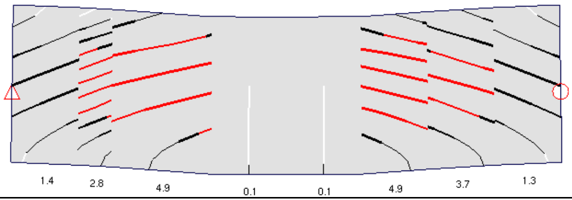
	Model 2 (Modified VecTor5)	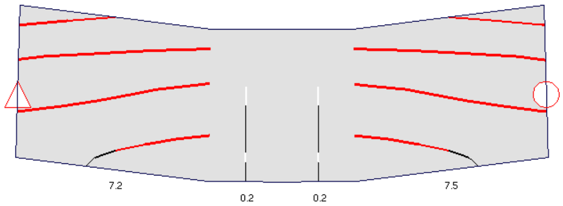
B-13-2	Model 1 (Original VecTor5)	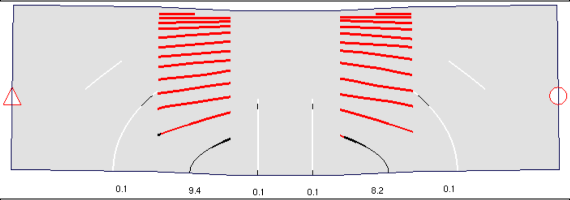
	Model 2 (Modified VecTor5)	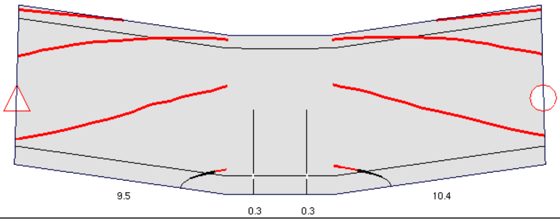
B15	Model 1 (Original VecTor5)	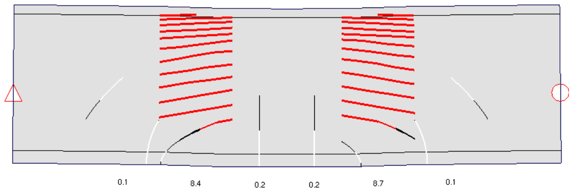
	Model 2 (Modified VecTor5)	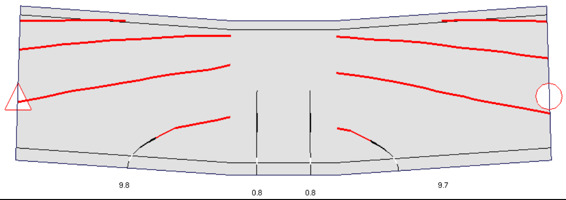
B17	Model 1 (Original VecTor5)	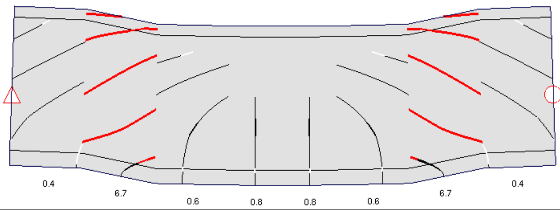
	Model 2 (Modified VecTor5)	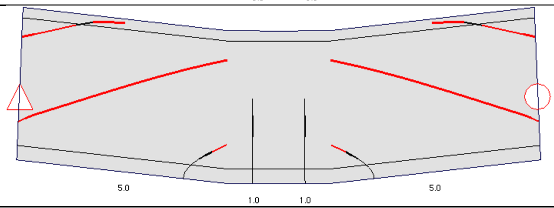

B18	Model 1 (Original VecTor5)	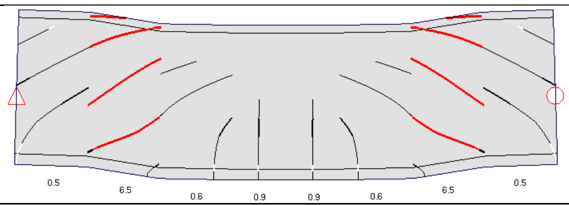
	Model 2 (Modified VecTor5)	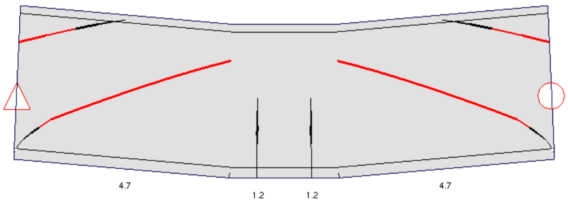

<u>Load-deflection responses</u>

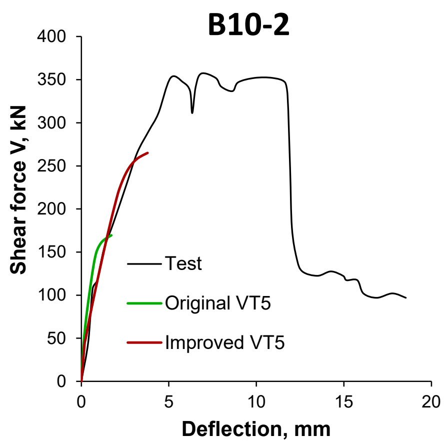

(a) Beam: B102

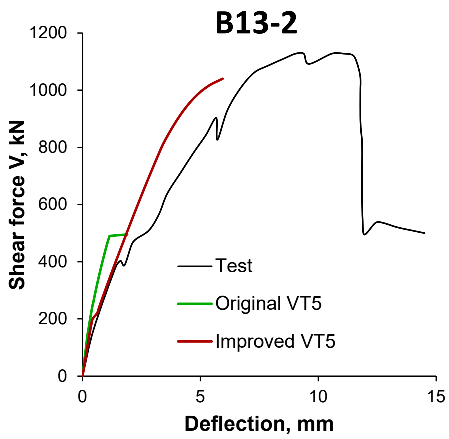

(b) Beam: B132

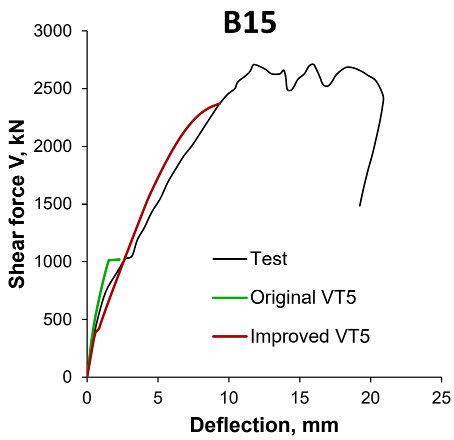

(c) Beam: B15

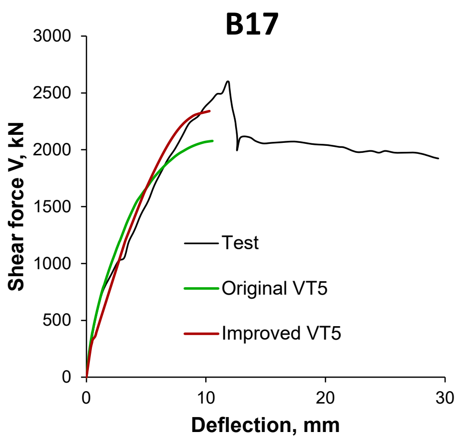

(d) Beam: B17

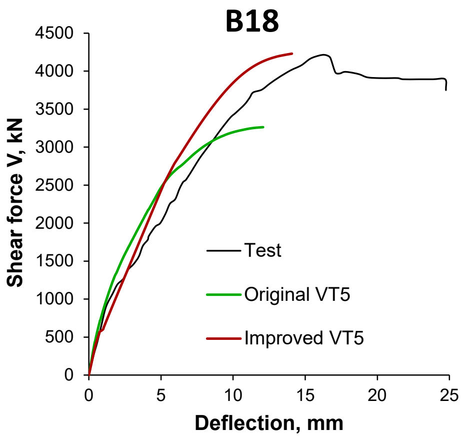

(e) Beam: B18

Figure 15 Load-displacement relationships

Convergence

The following shows the convergence for each beam. It should be noted only those from the improved VecTor5 are shown.

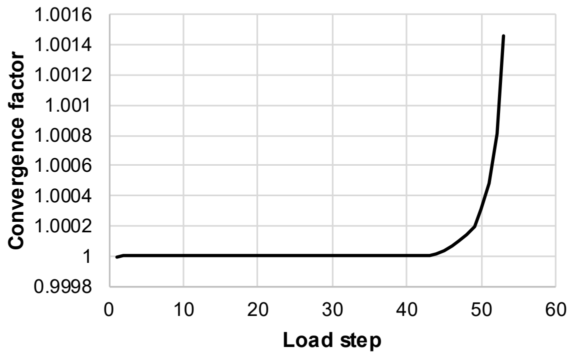

(a) Beam: B102

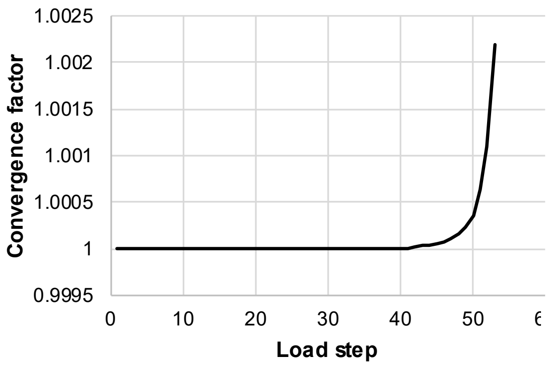

(b) Beam: B132

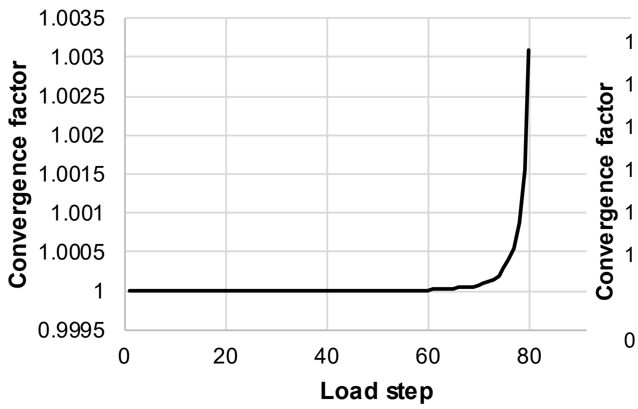

(c) Beam: B15

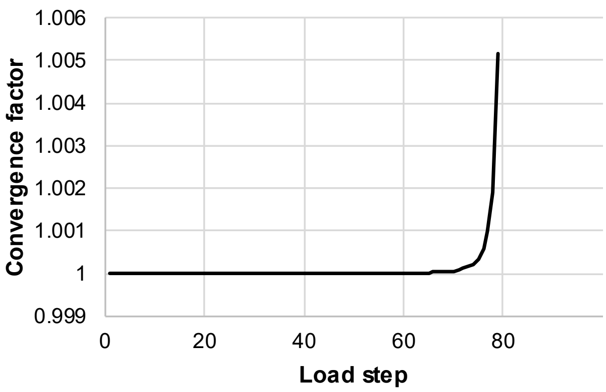

(d) Beam: B17

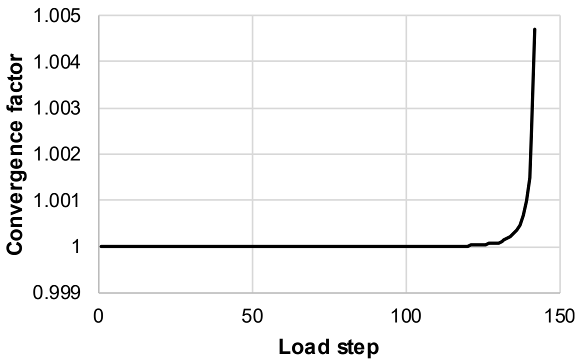

(e) Beam: B18

Figure 16 Convergence of Model 2 with modified VecTor5

Unbalanced force

The following shows the unbalanced force (N, V, M) in the corresponding axial force critical element, shear force critical element and bending moment critical element for each beam. It should be noted only those from modified VecTor5 are shown.

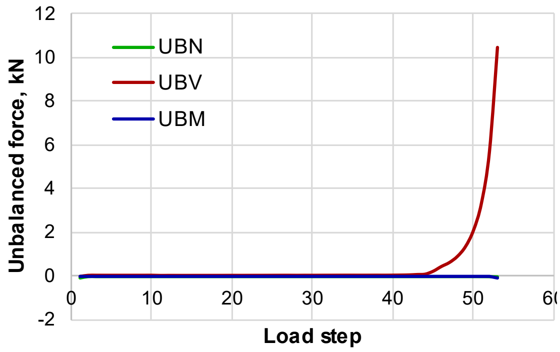

(a) Beam: B102

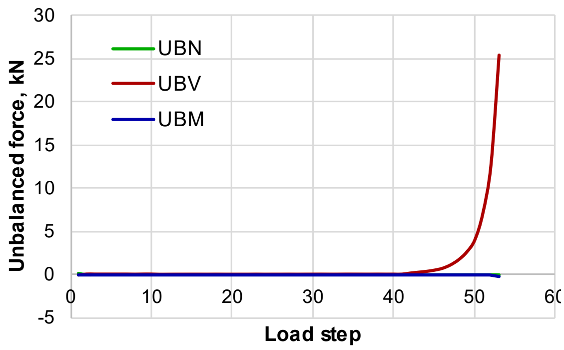

(b) Beam: B132

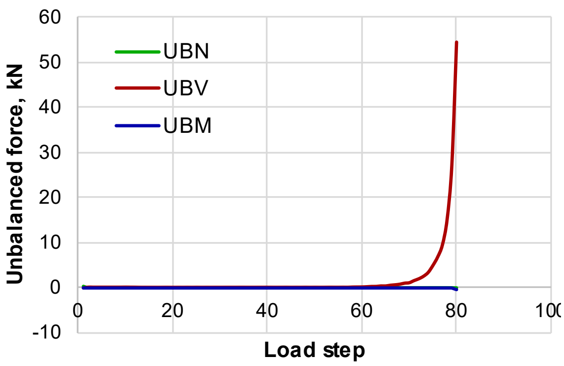

(c) Beam: B15

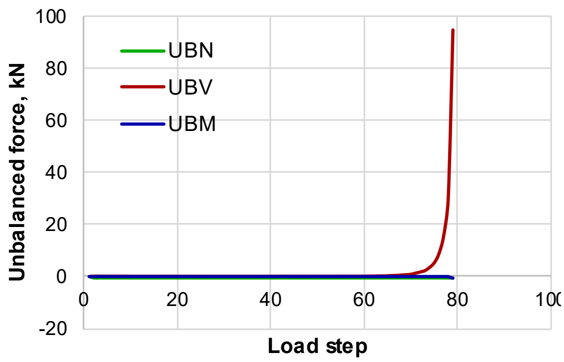

(d) Beam: B17

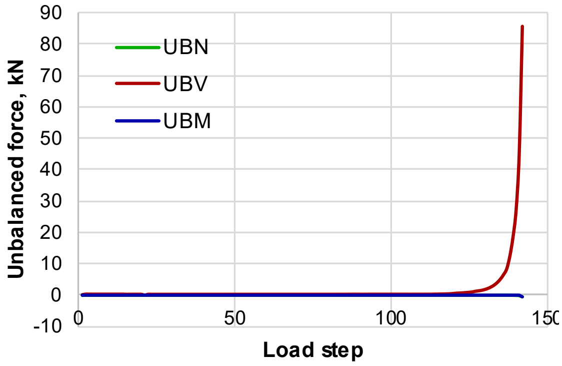

(e) Beam: B18

Figure 17 Unbalanced force of Model 2 with modified VecTor5

For all the beams, the unbalanced shear forces reach high values and increase monotonically, which means all the beams fail in shear.

<u>Calculation time</u>

Figure 18 shows the time distribution for each module of the Model 2 calculation. It is obvious that for all the 5 specimens, subroutine DPBM is the most time-consuming module. Therefore, it is necessary to make subroutine DPBM more efficient.

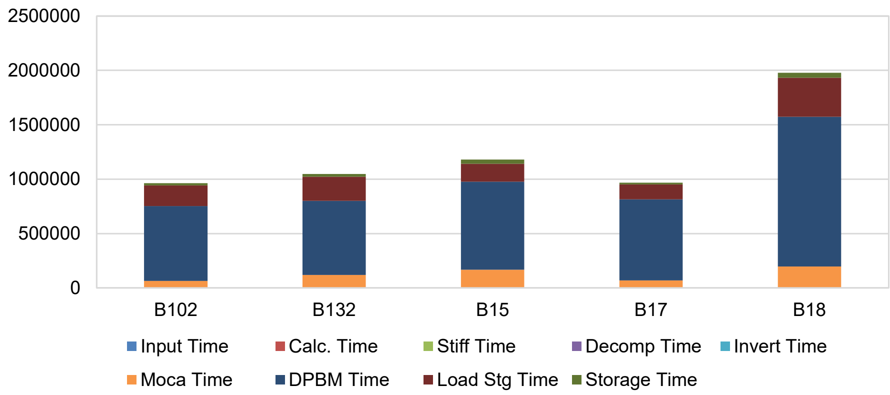

Figure 18 Calculation time of Model 2 with modified VecTor5

4) More efficient subroutine DPBM

Since the module of DPBM is rather time consuming therefore in this section, three measurements are taken to speed up subroutine DPBM.

<u>Subroutines eliminated:</u>

In the original subroutine DPBM, there are several subroutines included. The first attempt to speed up subroutine DPBM is to eliminate those subroutines and to include them as scripts directly in the main body of subroutine DPBM. Another issue is that even though subroutine DPBM is included in the framework of VecTor5 and it is meant to provide the internal forces of deep elements based on the nodal displacements, however, in case there will be error with the calculation for the whole structure, the subroutine MOCA in the original VecTor5 is still carried out to give the internal forces of deep element as well as other information based slender beam theory. Therefore, the total calculation time is expected reduced if MOCA is skipped and at the same time the calculation for the entire structure will not be disturbed. The calculation time distribution is listed in Figure 19.

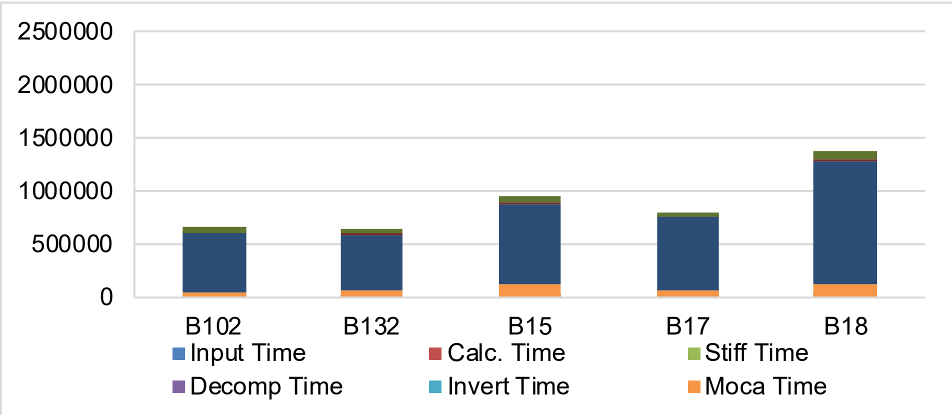

(a) Subroutine MOCA not skipped

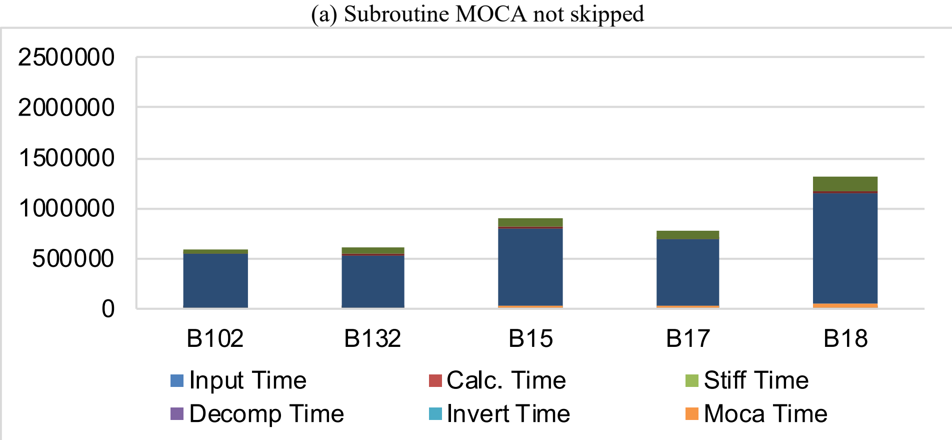

(b) Subroutine MOCA skipped

Figure 19 Calculation time of Model 2 with modified VecTor5: subroutines eliminated.

It is rather efficient to eliminate those subroutines included in subroutine DPBM to speed up the calculation, while the calculation time is less sensitive to the skipping of subroutine MOCA.

<u>Reduce the iteration number for concrete stress-strain relationship from 10002 to 2502.</u>

In subroutine DPBM to interpolate the concrete stress according to its strain, it is necessary to have a set of data storing the strain and stress along the concrete constitutive curve. In the original subroutine DPBM 10002 points are stored, and each time for the interpolation it takes large amount of time to find out the corresponding intervals for the strain and stress. Therefore, it is decided to reduce the number of points from 10001 to 2502 which can maintain the prediction as accurate as with 10001 points.

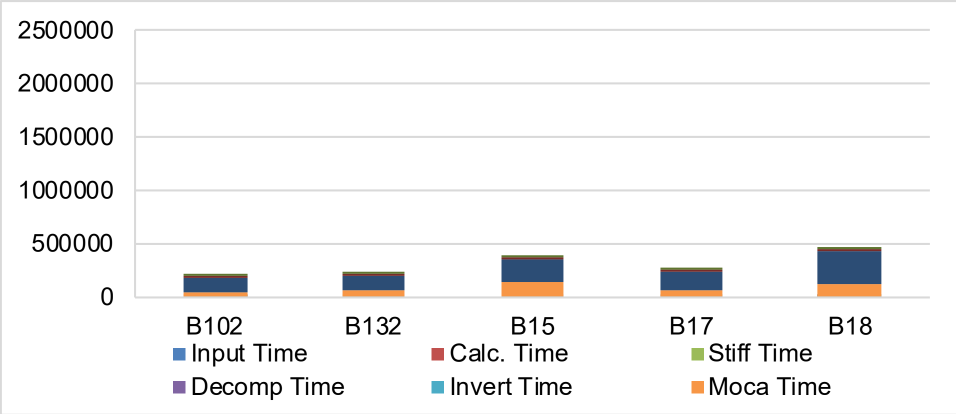

(a) Subroutine MOCA not skipped

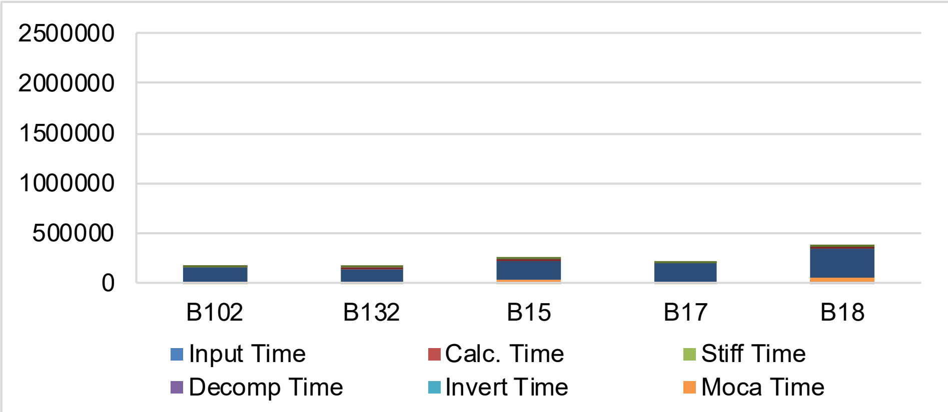

(b) Subroutine MOCA skipped

Figure 20 Calculation time of Model 2 with modified VecTor5: points number reduced for ε_c-σ_c

It can be seen from Figure 20b that after the three measurements implemented, the calculation time is reduced significantly. In the following study all the calculations are based on this improved subroutine DPBM.

4.1.2 2nd set of tests: Tanimura (2005)

The second group of specimens investigated are adopted from Tanimura (2005). These beams are also under symmetrical 4-point bending as in 4.1.1. The load-displacement response is shown in Figure 21.

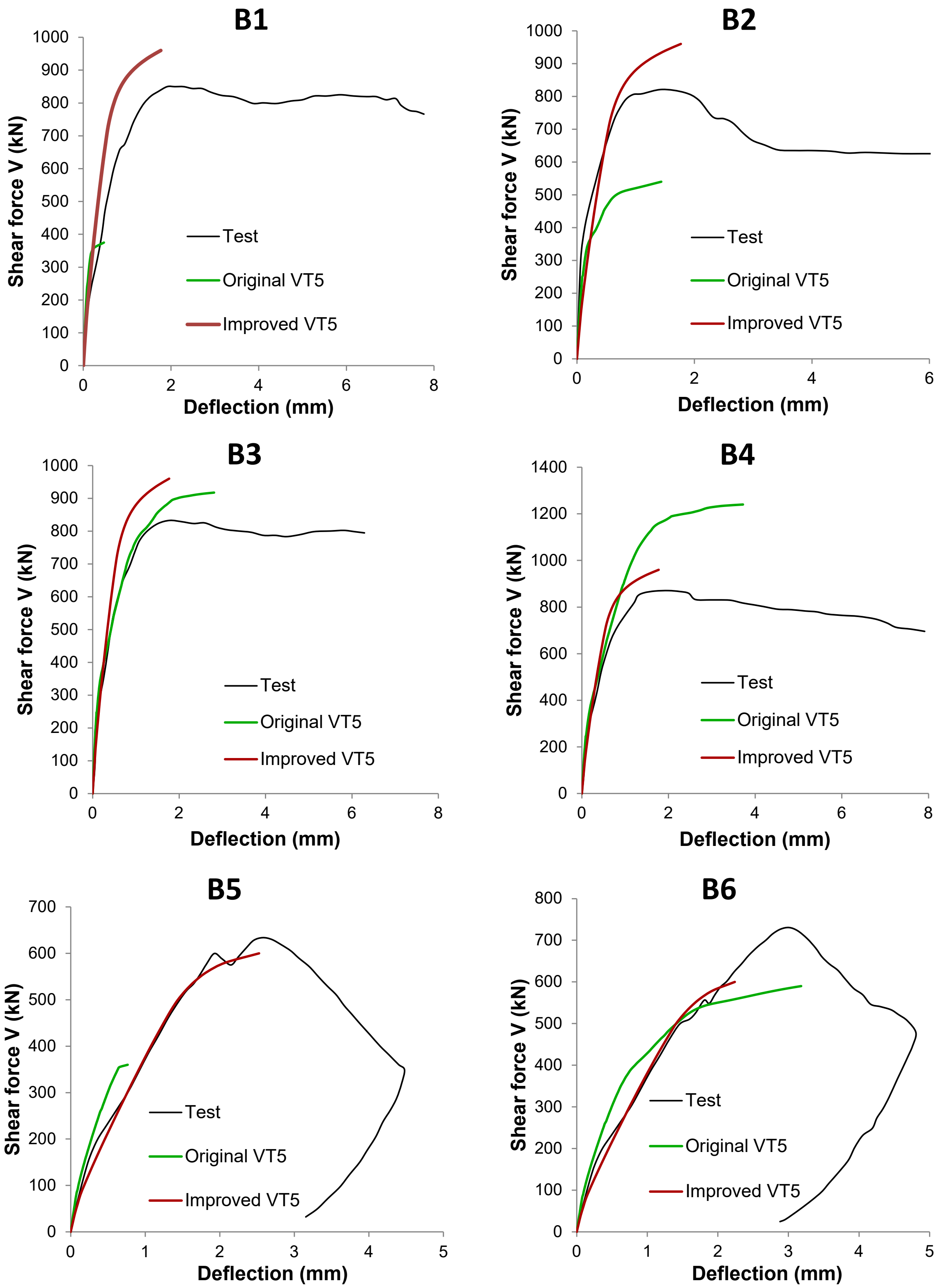
B1
Shear force V (kN)
Deflection (mm)
Test
Original VT5
Improved VT5
B2
Shear force V (kN)
Deflection (mm)
Test
Original VT5
Improved VT5
B3
Shear force V (kN)
Deflection (mm)
Test
Original VT5
Improved VT5
B4
Shear force V (kN)
Deflection (mm)
Test
Original VT5
Improved VT5
B5
Shear force V (kN)
Deflection (mm)
Test
Original VT5
Improved VT5
B6
Shear force V (kN)
Deflection (mm)
Test
Original VT5
Improved VT5

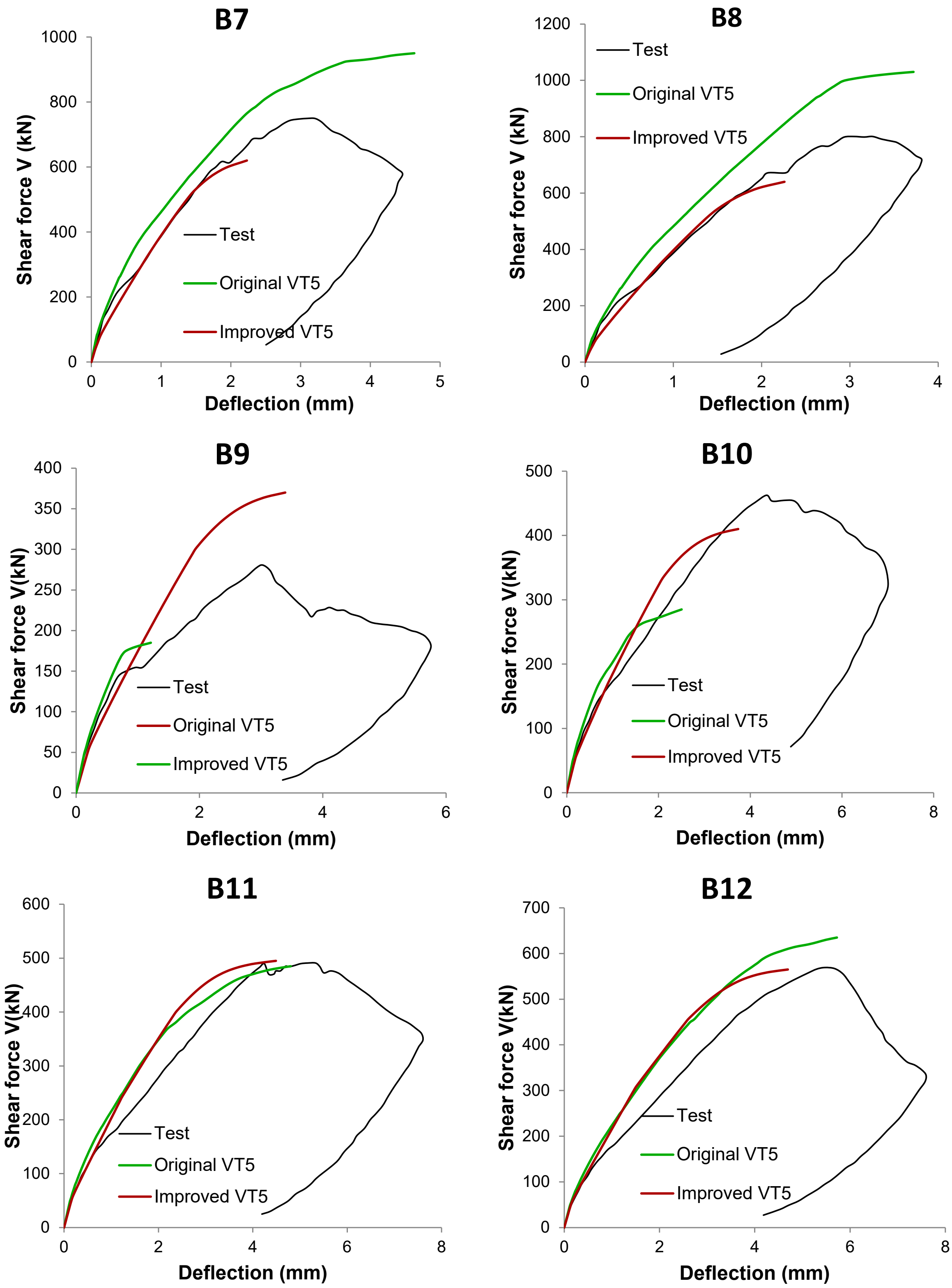

Figure 21 Load-displacement response of specimens from Tanimura (2005)

The results for the 12 beams from Tanimura (2005) show that the prediction from improved VecTor5, i.e., with subroutine DPBM included, are more reliable for various beam setups while the original VecTor5 either underestimate or overestimate the shear capacity.

4.2 Continuous deep beam

A continuous deep beam was tested in the University of Toronto in 2012 (Mihaylov et al., 2015), and the details of this beam are shown in Figure 22.

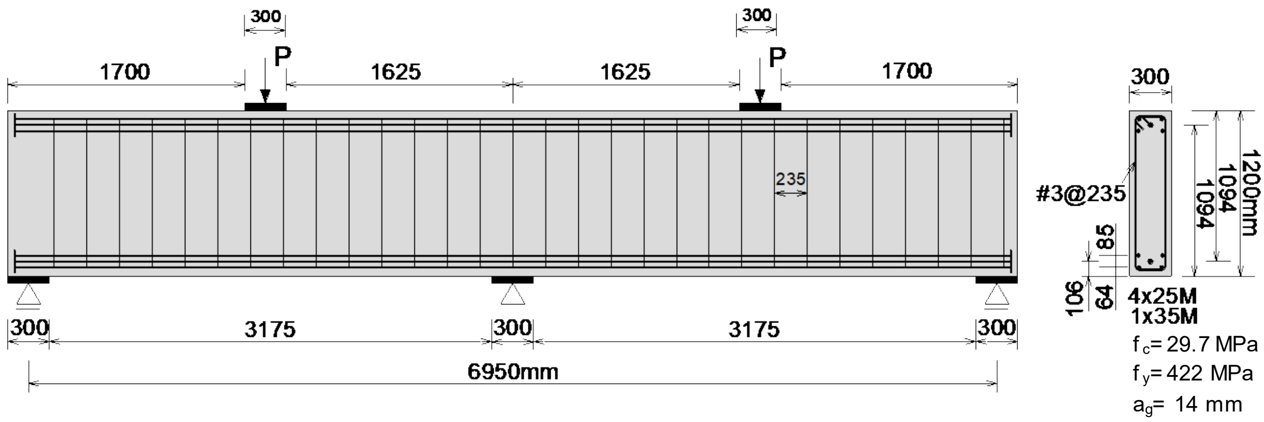

Figure 22 Continuous deep beam specimen

The predicted results from both original VecTor5 and improved VecTor5 as well as the experimental results are shown in Figure 23. It can be seen the prediction from the improved VecTor5 is closer to the experimental results compared with the original predictions.

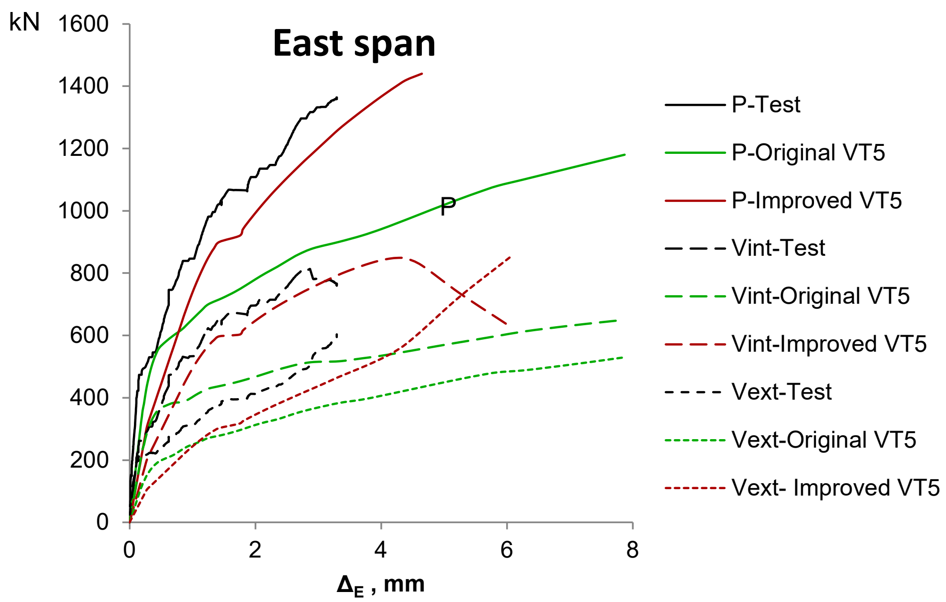

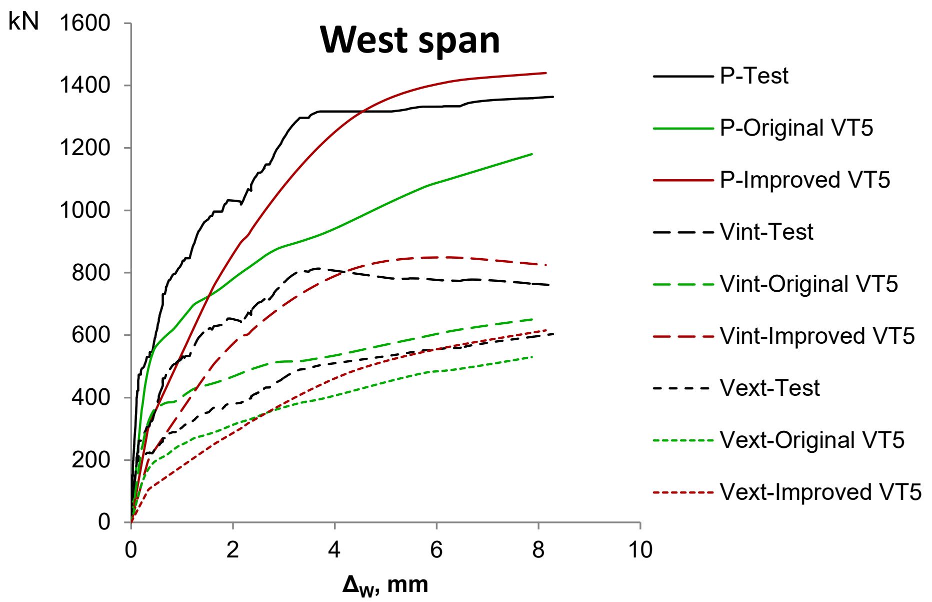

Figure 23 Load-displacement response of specimens from Tanimura (2005)

4.3 Frames

4.3.1 Two-story single-span frame

1) Comparison between predictions from VecTor2 and improved VecTor5

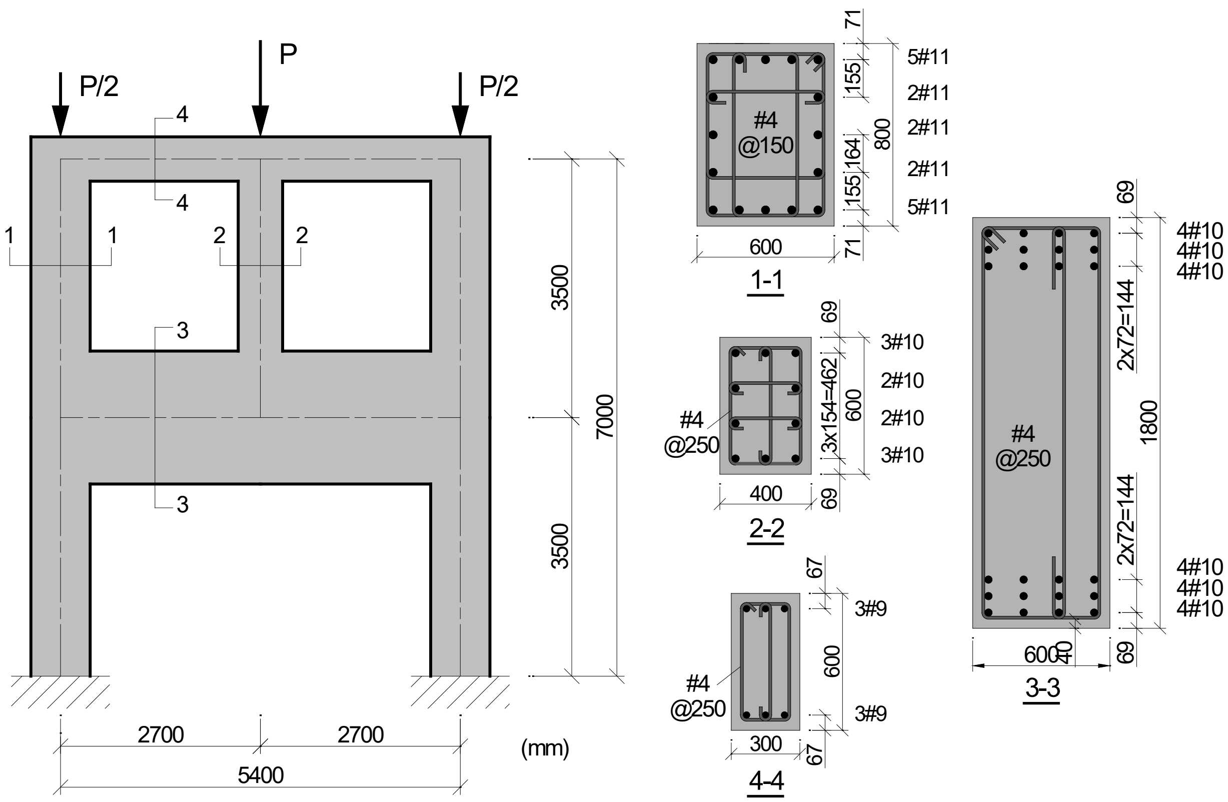

Figure 24 Two-story single-span frame

Table 4 Section properties

Section 1-1		
Longitudinal reinforcements		
φ_b, mm (#11)	35.81	≥ 8? yes!
A_{s0}, mm^2	1006	
b,mm	600	
h,mm	800	
A_c,mm^2	480000	
A_{smin}, mm^2	2400	
A_{smax}, mm^2	19200	
$n_{b,\ min}$	4	
n_b	16	
A_s, mm^2	16096	$\geq A_{smin}$? yes! $\leq A_{smax}$? yes!
ρ,%	3.4	
c,mm	40	
s_{bmax}, mm	152	
s_b, mm	112	$<s_{max}$? yes!
Transverse reinforcements		
φ_v, mm (#4)	12.7	
A_{sv0}, mm^2	129	
s_{vmax}, mm	573	
s_v, mm	150	$<s_{v,max}$? yes!

Section 2-2		
Longitudinal reinforcements		
φ, mm (#10)	32.26	≥ 8? yes!
A_{s0}, mm^2	819	
b,mm	400	
h,mm	600	
A_c,mm^2	240000	
A_{smin}, mm^2	1200	
A_{smax}, mm^2	9600	
n_b, min	4	
n_b	10	
A_s, mm^2	8190	$\geq A_{smin}$ yes! $\leq A_{smax}$ yes!
ρ,%	3.4	
c,mm	40	
s_{bmax}, mm	152	
s_b, mm	123	$<s_{max}$? yes!
Transverse reinforcements		
φ_v, mm (#4)	12.7	
A_{sv0}, mm^2	129	
s_{vmax}, mm	516	
s_v, mm	150	$<s_{v,max}$? yes!

Section 3-3		
Longitudinal reinforcements		
φ, mm (#10)	32.26	
A_{s0}, mm^2	819	
b,mm	600	
h,mm	1800	
f_c, MPa	28	
f_y,MPa	420	ASTM A615
f_u,MPa	620	
A_c,mm^2	1080000	
elongation	7-9%	
A_{smin}, mm^2	3600	
β_1	0.85	
$\rho_{balance}$, %	2.85068	
ρ_b, %	1.82	
A_s, mm^2	19656	
n_b	24	
c,mm	40	
$s_{bmin,}$mm	25.4	
s_b, mm		
Transverse reinforcements		
φ_v, mm (#4)	12.7	
A_{sv0}, mm^2		
s_{vmax}, mm		
s_v, mm	250	$<s_{v,max}$? Yes

Section 4-4		
Longitudinal reinforcements		
φ, mm (#9)	28.65	
A_{s0}, mm^2	645	
b,mm	300	
h,mm	600	
f_c, MPa	28	
f_y,MPa	420	ASTM A615
f_u,MPa	620	
A_c,mm^2	180000	
elongation	7-9%	
A_{smin}, mm^2	600	
β_1	0.85	
$\rho_{balance}$, %	2.85068	
ρ_b, %	2.15	
A_s, mm^2	3870	
n_b	6	
c,mm	40	
$s_{bmin,}$mm	25.4	
s_b, mm		
Transverse reinforcements		
φ_v, mm (#4)	12.7	
A_{sv0}, mm^2		
s_{vmax}, mm		
s_v, mm	250	$<s_{v,max}$? Yes

A two-story single-span frame is designed based ACI318_11, and the details are shown in Figure 24. Point loads are applied on top of the columns with P in themed-column and P/2 in the two side columns, respectively, simulating the real load case. There is a deep beam in this frame such that it is necessary to build a mixed-type frame model as shown in Figure 25. In this model the two shear spans of the deep beam are modelled with Type-8 nonlinear deep member and the rest are modelled with type-1 nonlinear frame member. It should be noted that the joints between deep beams and columns are modelled in the same way as suggested in the original VecTor5: type-1 nonlinear frame members are used within the joint zones and the steels in the member section are doubled for both longitudinal reinforcement and transverse reinforcement. Therefore, the deep elements are placed between two joints.

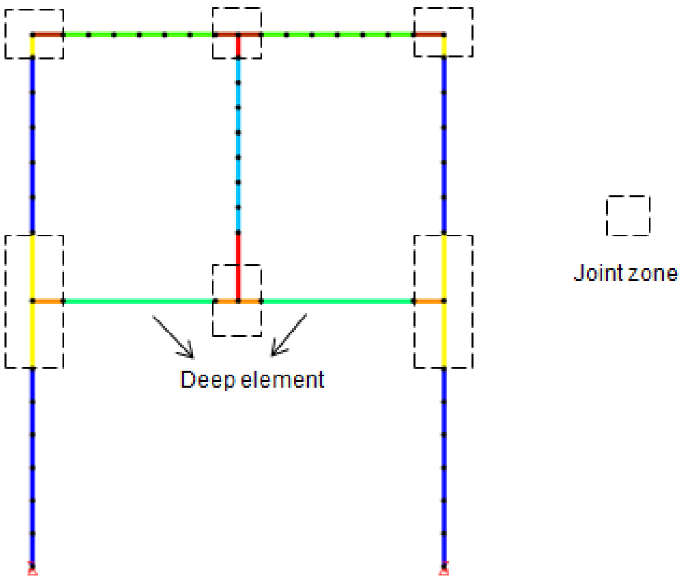

Figure 25 Model of a two-story single-span frame in improved VecTor5

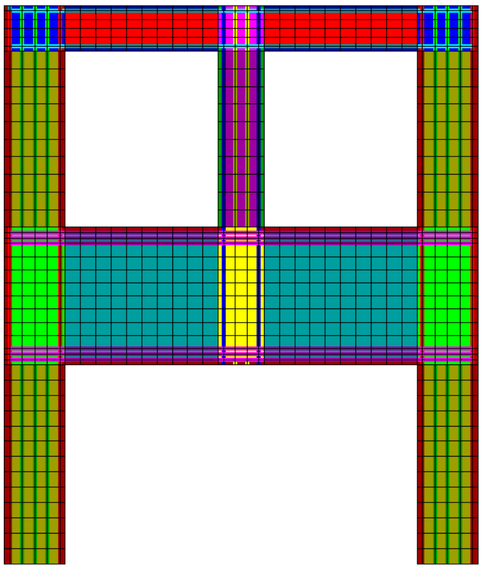

Figure 26 Model of a two-story single-span frame in VecTor2

Since there are no experimental results for this frame, an FEM analysis is carried out to get a reference for the prediction from VT5 to be compared with. VecTor2 is used for the FEM analysis and the model in VecTor2 is shown in Figure 26. It shows again (see Figure 27) that the improved VecTor5 provides a better prediction than original VecTor5 for shear-critical structures.

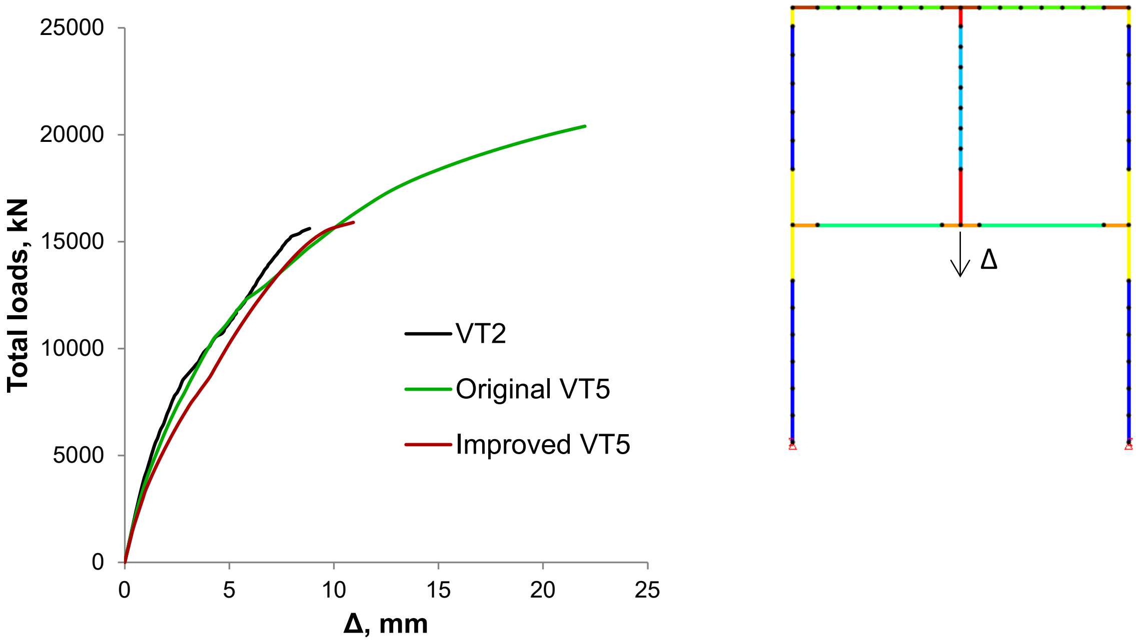

Figure 27 Shear response predictions of the frame

2) Effect of axial force on shear capacity of deep beams

However, it is noticed that the stiffness of the predicted result is lower than either predictions from VecTor2 or original VecTor5. This is due to the fact that in the improved VecTor5 the interaction between shear force and axial force is not taken into account. To demonstrate the benefits of axial force on the shear capacity of deep beams, simply supported deep beams with constant compressive loads (see Figure 28) is modelled in VecTor2 and the shear responses are shown in Figure 29. The stiffness increases under increasing axial load levels, which means that neglecting the interaction between axial force and shear capacity may underestimate stiffness in the shear response of the structure.

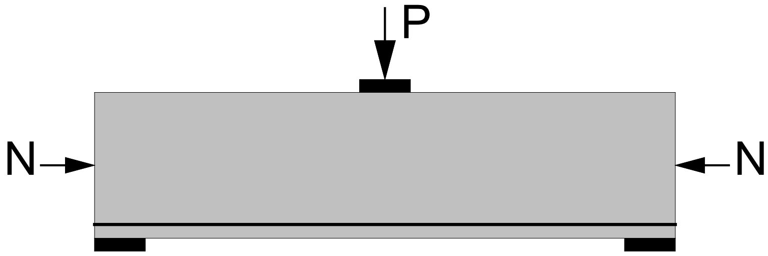

Figure 28 Deep beams used to study the effect of axial force on shear capacity.

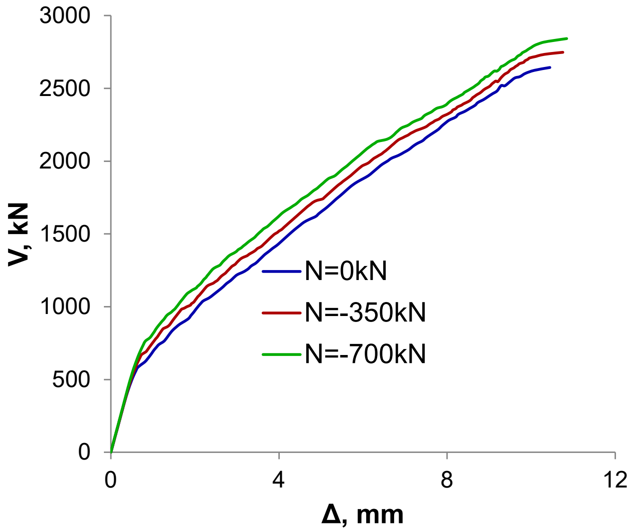

Figure 29 Deep beams used to study the effect of axial force on shear capacity.

4.3.2 Two-story two-bay frame

The frame in section 4.3.1 is extended to a two-story two-bay frame (see Figure 30). Similarly, the predictions from original VT5 and improved VT5 are compared in Figure 31.

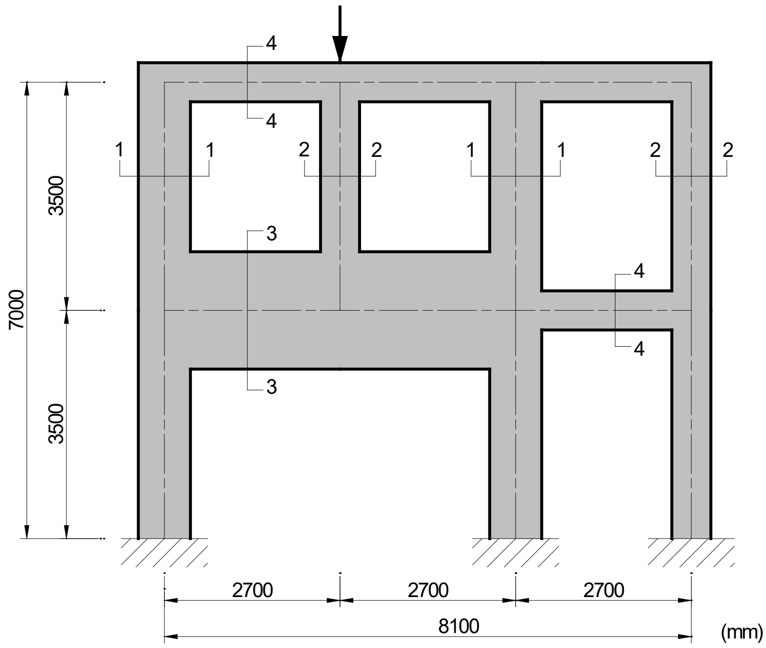

Figure 30 A two-story two-bay frame

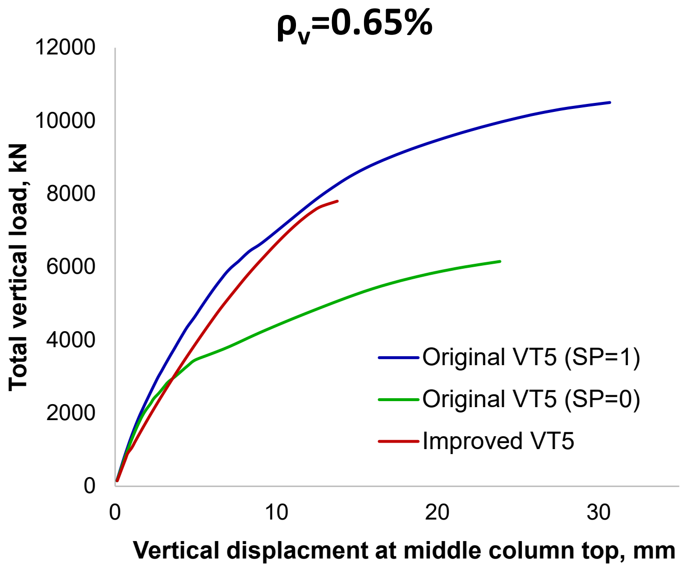

(a) Deep beam with stirrup ratio ρ_v=0.65%

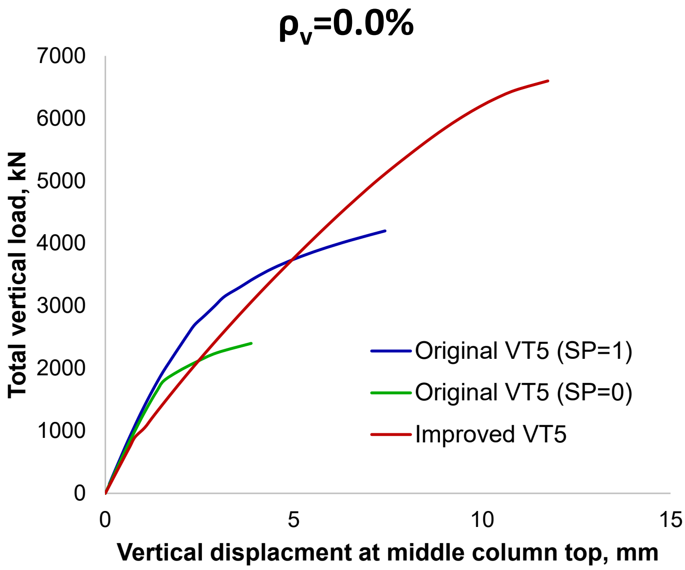

(b) Deep beam with stirrup ratio ρ_v=0.0%

Figure 31 Shear responses predicted with original VecTor5 and improved VecTor5.

4.3.3 Force control vs. displacement control

Since all the models mentioned above are loaded in the way of force-control, it is necessary to check if the improved VecTor5 can carry out displacement-control loading. A third frame is designed as shown in Figure 32. The results from both force-control loading and displacement-control loading are plotted in Figure 33. The two results coincide with each other in the pre-peak range, which means the improved VecTor5 is capable of both force-control and displacement-control loading.

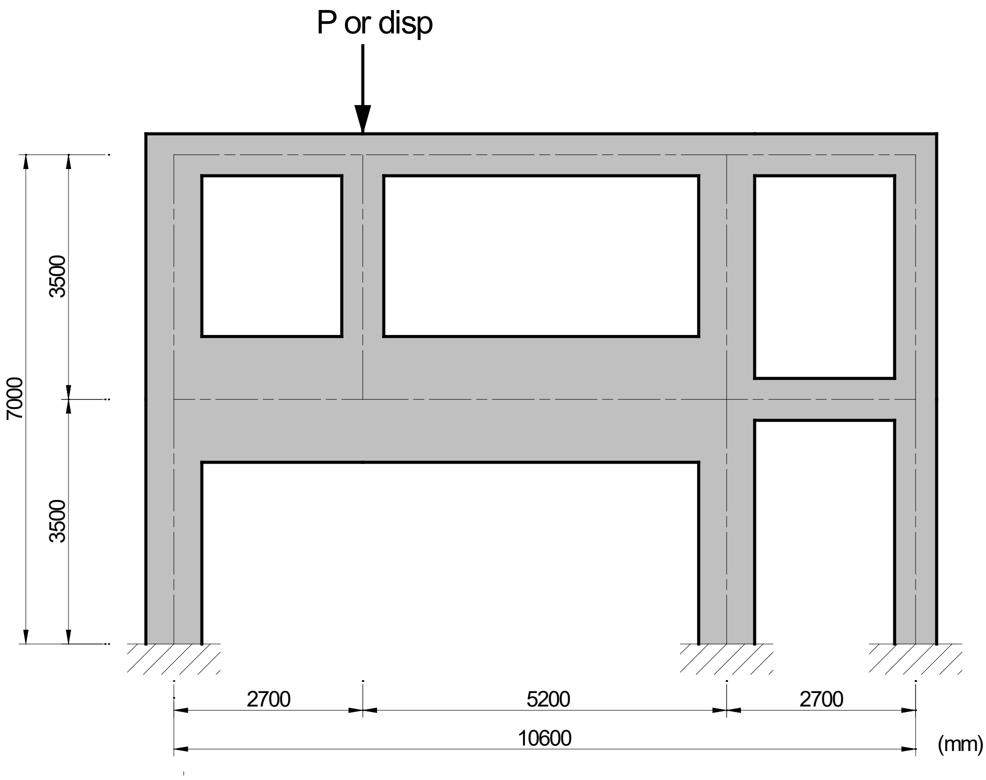

Figure 32 A two-story two-bay frame

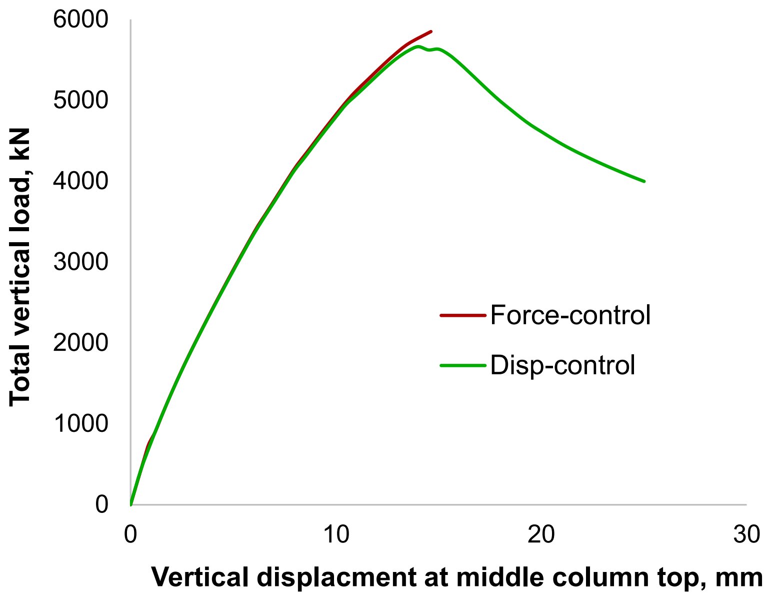

Figure 33 Shear responses under force-control loading and displacement-control loading.

5 Future Work

5.1 Axial force

As mentioned in Section 4.3.1, the interaction between axial force and shear response is not currently taken into account. Extended formulations should be developed and implemented to capture this interaction.

5.2 Unloading/reloading paths

Attempts were made to include unloading/reloading path for the three springs in the deep beam element. Due to some numerical problems, these are not included into the implementation. Future studies should investigate.

5.3 Automatic detection of deep beam elements

It could be useful for the user, if an automated algorithm detects all deep beam elements in a model. Such a feature could be included in future revisions. This work will also require automatically determining some or all input parameters required by VecTor. DPBM data file. The ones which could not be determined should still be input by the user.

5.4 Visualization of crack patterns in Janus

In Janus, the crack pattern views of deep beam elements have not been implemented. Undertaking this work will enable in depth visualization of the crack patters and help the user better interpret the analysis results.

6 References

Mihaylov, B.I., Hunt, B., Bentz, E. C. and Collins, M.P. (2015) "Three-parameter kinematic theory for shear behaviour of continuous deep beams," *ACI Structural Journal*, 112(1), pp. 47-57.

Salamy, M.,R., Kobayashi, H. and Unjoh, S. (2005) "Experimental and analytical study on RC deep beams", *Asian Journal of Civil Engineering* (AJCE), 6(5), pp. 409–422.

Tanimura, Y. and Sato, T. (2005), "Evaluation of shear strength of deep beams with stirrups", Quarterly Report of RTRI, 46(1), pp. 53-58.

The following is published after the preparation of this report, and contain more refined information.

Liu, J., Guner, S. and Mihaylov, B. (2019) "Mixed-Type Modeling of Structures with Slender and Deep Beam Elements" *ACI Structural Journal*, 116(4), pp. 253-264. <web link>

Annex 1: Flow chart of subroutine DPBM